SOFT ROBOTS

New soft robots really suck: Vacuum-powered systems empower diverse capabilities

Matthew A. Robertson and Jamie Paik*

We introduce a vacuum-powered soft pneumatic actuator (V-SPA) that leverages a single, shared vacuum power supply and enables complex soft robotic systems with multiple degrees of freedom (DoFs) and diverse functions. In addition to actuation, other utilities enabled by vacuum pressure include gripping and stiffening through granular media jamming, as well as direct suction adhesion to smooth surfaces, for manipulation or vertical fixation. We investigate the performance of the new actuator through direct characterization of a 3-DoF, plug-and-play V-SPA Module built from multiple V-SPAs and demonstrate the integration of different vacuum-enabled capabilities with a continuum-style robot platform outfitted with modular peripheral mechanisms. We show that these different vacuum-powered modules can be combined to achieve a variety of tasks—including multimodal locomotion, object manipulation, and stiffness tuning—to illustrate the utility and viability of vacuum as a singular alternative power source for soft pneumatic robots and not just a peripheral feature in itself. Our results highlight the effectiveness of V-SPAs in providing core soft robot capabilities and facilitating the consolidation of previously disparate subsystems for actuation and various specialized tasks, conducive to improving the compact design efficiency of larger, more complex multifunctional soft robotic systems.

INTRODUCTION

Robots that operate in highly variable environments or in close cooperation with humans require both robustness and adaptability to ensure reliability and safety. These features can be accommodated most easily by adding compliance to a robotic system, which can be achieved either actively through impedance control methods (*1*, *2*) or passively through compliant mechanical components and materials. In part, the advantage of a materials-based approach to creating compliant systems is to offload some of the burden of complexity in control to morphological and material computation, in a sense, to achieve robust and adaptable behavior (*3*, *4*). This latter strategy has been the recent focal point of the field of soft robotics, where inherently compliant and flexible materials such as silicone rubber are used to fabricate primary structural and active robot components (*5*). Various forms of soft pneumatic actuators (SPAs) powered by pneumatic pressure have been developed in this domain to complement the nature of these soft materials, which stretch and bend through inflation or deformation of elastic chambers to produce useful mechanical work (*6*–*16*).

This relatively new approach to robotics has yielded mobile platforms, manipulators, and other soft structures that are applicable in increasingly complex applications. Rough terrain locomotion, delicate handling, and human interaction tasks all benefit from the natural quality of SPA-driven systems to conform or yield safely to rigid environmental constraints without sacrificing the functional purpose of the device (*17*–*19*). Although now traditional soft pneumatic systems afford these benefits already using positive pressure, recent interest in negative pressure systems aims to improve these qualities further. Exploiting the effect of mechanical buckling to generate controlled force, vacuum-driven soft, muscle-like actuators have been successfully demonstrated using standard soft robotic materials and fabrication techniques (*20*, *21*). This type of actuator offers implicitly fail-safe operation, being limited by environmental pressure from actuating beyond a maximum force and displacement, and directly enables contractile motion, more similar to biological muscle than the expansion-based motions of many positive pressure-driven soft actuators.

Following previous efforts (*20*, *21*), we introduce a vacuum-powered SPA, the V-SPA, to expand the diversity and utility of this versatile power source for new soft robots. In comparison with the few existing examples of vacuum-driven actuators, this new type of actuator is exceptionally rapid to fabricate for proficient iteration through multiple designs. This is a result of requiring no molds or sacrificial compounds and being constructed primarily of readily available, manufactured foam sheets. The use of porous foam structures in soft robotics has recently been investigated to a limited extent for various novel benefits. With self-manufactured poroelastic foam, a bioinspired fluid pump was developed to showcase the utility and simplicity of foam-based compliant actuation (*22*). Following a similar method to fabricate poroelastic foam from a moldable compound infused with a fugitive salt porogen, highly customized inflatable structures can be sculpted in free form for laboratory, art, or classroom educational purposes (*23*). Other work has explored the use of bicontinuous metal-elastomeric foam to achieve variable stiffness and self-healing properties (*24*). Although most of these methods have been applied toward the fabrication of SPA devices powered by positive pressurized air, the application of vacuum to foam structures is an approach that combines the advantages of vacuum power with some of those inherited from the properties of the foam material itself, including impact resistance, robustness, and storage-friendly "crushability" (*25*). Our soft actuator exploits this combination, enabling a wide range of soft robotic applications, including safe, lightweight, wearable devices, collaborative machines, or packable mobile robots that are space- and energy-efficient, suitable for remote deployment or even possibly flight (see Fig. 1).

Capitalizing on the vacuum supply available for actuation, vacuum-based soft robotic systems can also leverage this source to incorporate other functions and features powered by negative pressure, without the need for an additional power supply or additional subsystem infrastructure. Vacuum-powered mechanisms have been shown to

Reconfigurable Robotics Laboratory, École Polytechnique Fédérale de Lausanne, 1015 Lausanne, Switzerland.
*Corresponding author. Email: jamie.paik@epfl.ch

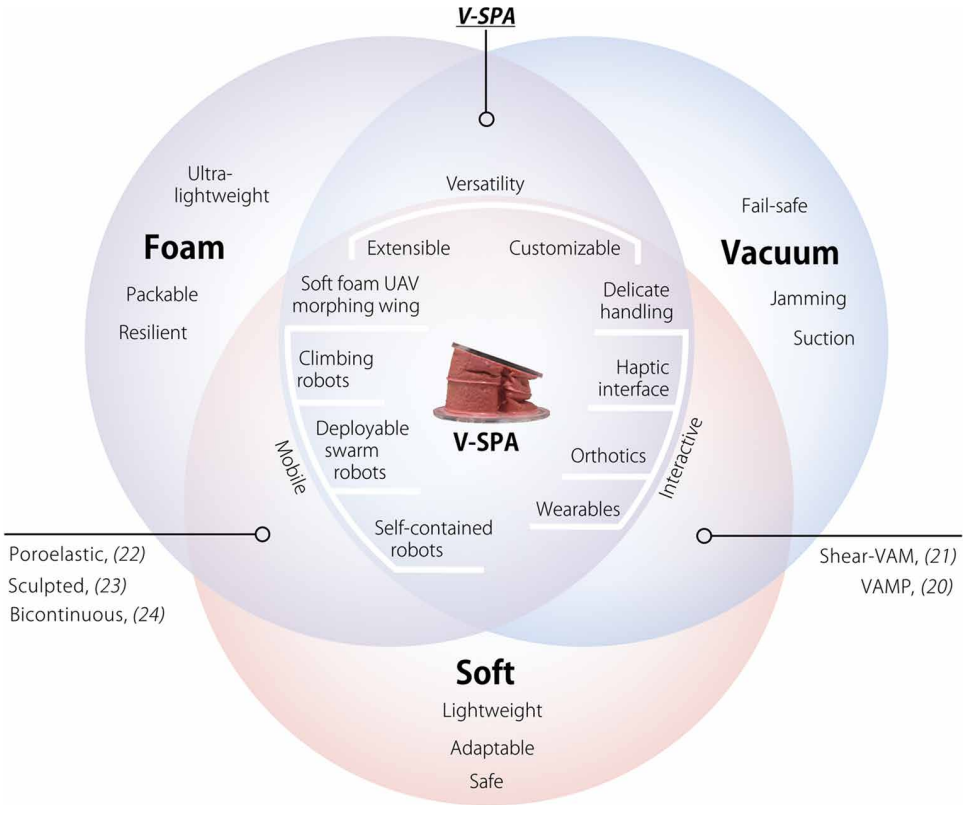

Fig. 1. V-SPAs blend multiple material and operational domains for diverse potential applications. Existing work explored the use of vacuum and foam materials separately for the development of soft robotic systems to leverage the unique attributes of robustness, safety, and manufacturability offered by different fabrication and actuation methods. This work explores a new approach that leverages foam and vacuum power simultaneously with an actuator called the V-SPA to take advantage of a new construction technique that enables rapid production of soft robotic systems using minimal resources and opens the possibility for fully vacuum-powered systems that enable soft robots with expanded capabilities.

enable operations useful to soft robots, including gripping (*26*), suction (*27*), and stiffness tuning (*28*–*31*). By adding a lightweight alternative for actuation to this variety of available vacuum-driven mechanisms, V-SPAs open the opportunity to expand the capability of soft robots while actually minimizing the size and complexity of their design and implementation. The seamless integration of these mechanisms through a common vacuum supply not only yields more efficient soft robot design but also subsequently facilitates high-order soft pneumatic systems with many degrees of freedom (DoFs), which are still relatively scarce in the field of soft robotics. To demonstrate this facility, we use V-SPAs in a typically complex and difficult multi-DoF robot morphology, generally referred to as a continuum robot. Also known as hyper-redundant robot manipulators, trunks, tentacles, or snakes, these narrow structures often consist of a linear chain of repeating modular units, each with single or multiple active DoFs. This concept enables a high degree of kinematic maneuverability and flexibility for either manipulation (*32*–*36*), positioning (*31*, *37*), or locomotion (*38*–*40*) tasks to account for variable environments or system objectives. Although the low mass of the V-SPAs themselves makes such an architecture with many DoFs more feasible, dealing with the practical difficulty imposed by cumbersome, overlapping pneumatic supply lines routed from a central control source to many independent actuator units often limits its realistic execution. To overcome this barrier and allow the consolidation of multiple vacuum-based mechanisms into the same platform through a common vacuum supply line, we used a decentralized, modular design approach.

This work validates the integration of our actuator in multifunctional vacuum-driven soft robotic systems by experimental demonstration of interaction task versatility and mechanical performance tuning of physical properties through the use of plug-and-play control and design methods. By introducing actuation technology and demonstrating the combination of different functions made possible through a negative pressure pneumatic power supply, we help to establish vacuum power as a substantial alternative class of soft robotics that offers unique and important potential for realizing complex and advanced systems.

RESULTS

Vacuum-powered soft pneumatic actuator

We designed and developed a critical robotic component, the V-SPA, which is characterized by its implicit reliability and safety through the utilization of vacuum power and the robust properties of a foam core. This new actuator is simple in design and easy to fabricate without the need for either an internal or an external mold. It is composed of a laser-cut, off-the-shelf foam core and thin, brushed-on layers of silicone rubber and can be manufactured from scratch—ready to be used in less than 2 hours. The foam core acts as an internal scaffold over which uncured silicone rubber can be applied to form a thin, sealing layer around the open-celled foam, as can be seen in fig. S1. This creates an enclosed, airtight structure that is only sparsely filled with soft, porous material. Whereas conventional SPAs or other vacuum actuator designs feature completely hollow inner cavities, the use of foam allows the wall thickness of V-SPAs to be much thinner because it provides much of the structural support typically given by a thicker wall needed to maintain a nominal actuator shape. This difference in material wall thickness helps to offset the added mass of the core, yielding an ultimately lighter weight actuator overall. Upon activation, vacuum is applied to the internal volume through a supply channel, and the entire V-SPA structure collapses inward to produce tensile force that can be used for actuation. The low-density core is easily deformed and crushed when vacuum is applied but immediately provides elastic return in conjunction with the elasticity of the outer silicone membrane after actuation to return the actuator to its original shape. The activation of a circular V-SPA array can be seen in movie S1.

In soft robotics, foam-based vacuum-powered actuators offer a solution to improve the efficiency of soft systems, by reducing mass in actuators, allowing for the integration of additional mass components

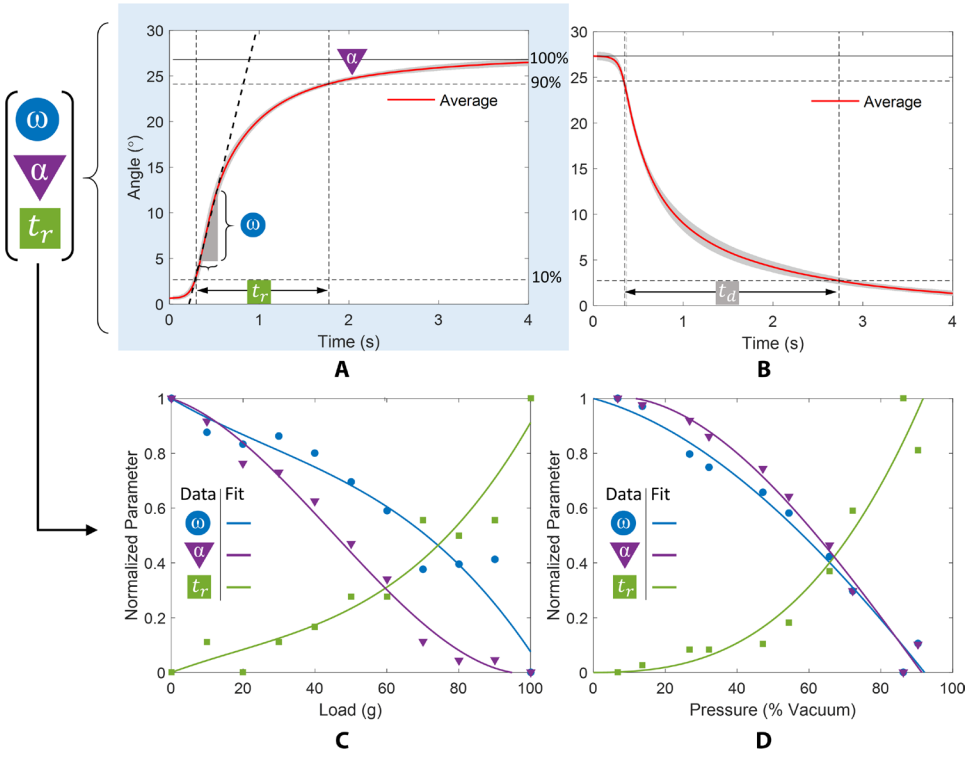

Fig. 2. V-SPA Module step response characterization. Three V-SPAs were characterized with a step input while measuring the angular response with an inertial measurement unit (IMU). The average (red curve) step response at maximum vacuum with no load is shown in (**A**), and the step-down profile is shown in (**B**). A single SD is also shown in light gray shading, for 30 cycles (10 cycles for each of three actuators) comprising the average response. The metrics found from the average step response for variable loads are shown in (**C**) and variable pressure in (**D**), and the trends were plotted with a third-order polynomial fit.

onboard to enable fully self-contained systems, including batteries and pressure (or direct vacuum)–generating pumps. This reduction in the total system mass budget also makes room for larger systems with more DoFs, enabling further complex behavior. Although vacuum power is not suited for every application, in part due to limited force production at atmospheric pressure, for use at small scales where this force limit is perhaps beyond maximum requirements, and where this limit offers a unique safety feature because it prevents actuating beyond the force imposed by external pressure, V-SPAs hold a unique advantage at substantially low cost in weight, materials, and production effort.

Scalable, reconfigurable soft robot

We developed a robotic platform using V-SPAs to power hybrid (*41*) modular units, known as V-SPA Modules, which contain both soft actuators and rigid components necessary for their power and control. This architecture was chosen to practically implement V-SPAs in an example soft robotic system with enhanced and diverse capabilities. The modular design of the units enables rapid, simplified restructuring and control of various robot configurations for easy testing and validation of vacuum system extensibility. Specifically, these modules allow the addition or subtraction of mechanical DoFs with little or no physical design effort through standardized pneumatic and electrical network connection ports. Other peripheral device modules with different functionalities can also be easily combined with the actuators in the same way. To eliminate the effort of developing customized control for each unique combination of modules in a scalable or multifunctional system, we use a standard control scheme that does not change with the number or type of modules connected. Although high-level control planning and programming is still required to achieve specific tasks, the low-level management of multimodule integration is automatically taken care of through this flexible plug-and-play network architecture using embedded control circuitry and hardware. By following this design approach, the resulting reconfigurable soft robotic system we produced embodies a typically challenging morphology, a hyper-redundant continuum-type robot not easily reproduced by other existing soft robot design methods.

V-SPA Module configuration

We produced V-SPA Modules using three actuators each, evenly spaced in a cylindrical configuration and connected at the top and bottom to rigid plates that house or mount electronics, valves, pneumatic fittings, electrical connectors, and distribution channels connecting to a centralized vacuum supply line. Other work has leveraged this approach for more efficient configuration of mobile snake-like robots (*42*, *43*) and use in a surgical continuum robot composed of a serial chain of 3-DoF soft actuator modules with miniature control valves embedded locally (*44*). Our V-SPA Modules similarly exploit the advantages of decentralized hardware architecture to reduce complexity, space, and weight of vacuum-powered systems with integrated peripheral functions.

The three V-SPAs comprising each module are used to tilt the orientation of a rigid upper plate [conventional printed circuit board (PCB)] relative to the one at the bottom. The actuators are attached to these end plates and contract when activated, leading to angular deflection between them in a direction and degree defined by the combination of actuators activated simultaneously and the magnitude of their activation (by duty cycle, proportional to length). With a purely binary scheme to control the actuators fully on or off, the module actuators can be triggered independently or in pairs to produce six unique directions of motion at a fixed angle of deflection. The coactivation of all three actuators does not produce significant linear deflection as implemented here with a stiff supply conduit through the center, but this motion can easily be achieved without it. The motion of a V-SPA Module following this simple control method can be seen in movie S2. A more complex activation of the actuators is not shown here but can be accomplished using pulse-width modulation (PWM) control for each actuator to achieve variable contraction, expanding the workspace to continuous, 360° directed bending with variable angle. Although the angular deflection of the module can be represented as combined rotations along two axes in space, we express this in terms of active DoF, rather than spatial, to define each V-SPA Module as a 3-DoF actuated joint. Characterization testing of the V-SPA

Modules presented in Fig. 2 was performed by measuring the angular step response of a module under varied conditions. From the different response profiles, metrics were obtained relating actuator and module performance to different loading and supply pressure conditions. The measured characteristics are summarized in Table 1.

Each V-SPA Module connects in series to another through connections on the top and bottom to a central pneumatic supply line, power and ground lines, and communication bus, shown in Fig. 3A. The overall structure of the resulting network of modules can be seen in Fig. 3B with the note that this architecture is not only limited to efficiently integrating actuators alone but also designed to facilitate rapid and simple extension of many different module types for vacuum (or other) pneumatic robotic systems. Commands to individual actuators in each networked module are relayed over a communication signal line using a robust serial protocol designed initially for low-cost red-green-blue (RGB) light-emitting diode (LED) serial displays. Because each channel of every module in the network is identified sequentially and not through a unique address, this allows modules to be added or subtracted in a generic way that does not affect the low-level control programming. Although such modules could be used in various combinations, in a multitude of different robot topologies, the nominal configuration studied here in direct linear arrangement allowed for the demonstration of many interesting features enabled by V-SPAs and vacuum power alike.

Hyper-redundant soft robot performance

We first tested the operation of a five-module robot to quantify its performance in the simplest form, as a soft manipulator arm. The workspace and repeatability of the robot's three principle directions of motion from an initially vertical standing orientation were measured using an external OptiTrack motion capture system to demonstrate the practical utility of a V-SPA–based system. The proximal end of the robot was fixed to a stationary base, and three markers were attached to the distal end to track the three-dimensional (3D) trajectory of their centroid, treated as the robot end point. For this preliminary evaluation, every module in the robot was synchronized to move the end point virtual marker through three distinct locations (roughly 0°, 120°, and 240°) representing the robot's principle directions of motion, as shown in Fig. 4A. Binary activation signals (on/off) were used to achieve the maximum bend in each of these directions, although independent control of each of the 15 total V-SPAs in the robot (three per module) is possible, and continuous motion of each actuator or combination of actuators in a single module could also be achieved using PWM signals to produce motion in any arbitrary angular direction.

The robot end point position was measured for 10 cycles through each location, and a 2D error ellipse (95% confidence interval) was calculated for each set of 10 points in each of the three locations (see movie S3 for a video of the 10-cycle trial test). The length of the ellipse major axes, corresponding to the largest variability in end point positioning, was averaged for all three locations. For a five-module robot, the average error recorded across the three principal locations tested was found to be ±3.4 mm. This corresponds to an average repeatability measure of ±0.68-mm accuracy per module. Individually, the range of accuracy across each of the three respective directions differed slightly as a result of variable construction and individual actuator performance, with the lowest variability in a particular direction (actuator 3) measured to be ±1.9 mm for the robot as a whole or ± 0.38 mm per module along that axis. Although the path and final position of the robot end point in each direction are seen to be repeatable, deviations from a purely linear path (from the top view) between the neutral start point and end points can also be seen. In part, this is because the actuators are driven by the inherently unstable mode of buckling of the V-SPA outer rubber skin made variable between actuators by nonuniformity in their construction and materials. Despite this variability from manual fabrication, these measurements validate the use of V-SPAs for highly repeatable tasks critical for practical robotic systems.

Validation of reconfigurable soft robot capabilities

To complement the mechanical flexibility of the hyper-redundant robot, we can easily integrate a variety of module types with it to achieve design and task flexibility. Possibilities for vacuum-driven systems include those shown in Fig. 4B. Three of the modules depicted are demonstrated in this work, whereas future modules yet to be implemented are proposed to further illustrate the capacity and utility of vacuum-based soft robot design. We validate the diverse functionalities facilitated by these modules through demonstration of various interaction tasks between the robot and its environment and an example of controllable mechanical tuning of dynamic system properties implemented through a plug-and-play modular design paradigm. Through the use of peripheral modules, these abilities extend the

Table 1. Physical properties and performance of V-SPA Module. Performance metrics were estimated from an angular displacement step response test recorded relative to gravity using an IMU fixed to the upper stage of the module and with 86.2% vacuum supply.

Properties	Value	Unit
Size ($D \times H$)	45 × 45	(mm)
Total module weight	45.0	(g)
V-SPAs (×3)	11.1	(g)
Solenoid valves (×3)	12.0	(g)
PCBs	8.5	(g)
Acrylic and epoxy layers	8.5	(g)
Central conduit (tubes, connectors, wires)	4.9	(g)
Blocked torque	166.9	(N·mm)
Specific torque (relative to actuator mass)	45.1	(N·mm/g)
Angular velocity, ω (no load)	3.5	(°/s)
Step rise time, t_r	1.5	(s)
Step decay time, t_d	2.4	(s)
Bandwidth	0.2	(Hz)
Maximum angular stroke, α (no load)	27.3	(°)
Specific power (relative to actuator mass)	5.0	(W/kg)
Specific energy (relative to actuator mass)	1.2	(J/kg)

diversity of applications for soft robots, including enhanced mobility and controllability enabled by the configurations depicted in Fig. 4C, highlighting the efficacy and versatility of V-SPAs and vacuum-based soft robotic systems as a whole.

Interaction task: Suction manipulation

As a first test of the versatility of the vacuum power supply, a suction manipulator component was added to the end of the positioning arm, maintaining a modular design approach. A snap-fit 3D printed part was attached to the distal robot module to provide the structural basis of the suction module, including a modified off-the-shelf soft suction cup. The new peripheral module was connected to the shared vacuum power supply, and a custom networked control valve was plugged in series to the output electrical interface of the distal actuator module to be controlled along the common control signal bus. A silicon tube connected the valve output to the internal volume of a soft suction cup through a hole at the top, enabling it to be actively depressurized or vented to the atmosphere for controllable attachment or detachment to objects. The soft continuum manipulator arm was then tested in a simple reaching and manipulation task of smooth acrylic containers to demonstrate the performance of combined actuation and suction manipulation. The multifunctional system was able to successfully "grasp" and relocate objects from a starting location to target bins, as shown in movie S4.

Interaction task: Vertical window climbing

Integrating lightweight actuation with other vacuum-based mechanisms enables capabilities beyond positioning and manipulation tasks. We demonstrate further the advantages to combining these mechanisms by reconfiguring V-SPA Modules and suction cup modules into a soft robot capable of vertical climbing on smooth surfaces. The actuator and architecture previously presented readily accommodated two vital requirements for this type of robot: to provide active motion for climbing and selective attachment and release of robot footholds while maintaining low enough weight to not hinder the effect of those capabilities. The low-mass foam core V-SPAs are naturally well suited to this application, and the modular, shared vacuum supply architecture of the complete soft robotic system enables the efficient integration of the active functions necessary for vertical climbing in a nearly self-contained soft robotic system that can scale surfaces such as glass windows. With only an open-loop, fixed-gait pattern controller and without optimizing timing parameters to find the maximum speed, demonstrated gait was measured to be 2 mm/s or 0.01 body lengths per second (BL/s). Although the climbing robot we present here lacks an onboard electrical power supply and pneumatic vacuum generation source, we verified that it is capable of carrying an additional payload up to 70 g, which may be useful for accommodating the remaining components to enable a more autonomous robot in the future. Figure 5A shows the progression of the climbing robot, and movie S5 shows testing with increasing external payload, with an evident corresponding reduction in climbing speed. Although this change in climbing performance can be attributed

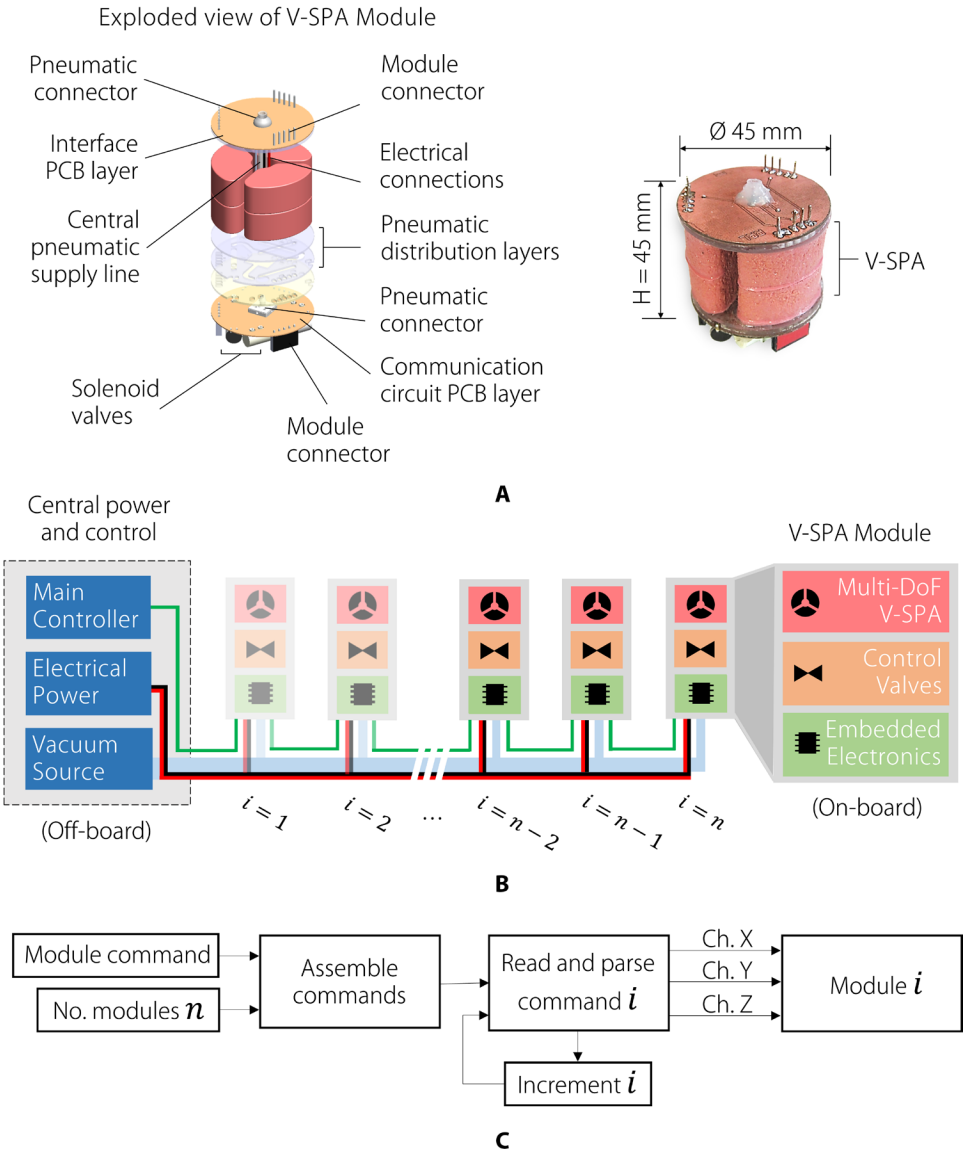

Fig. 3. Architecture of V-SPA Module and integrated soft modular device network. (**A**) Each module contains three main components: actuators (V-SPA), control valves, and electronics. (**B**) Each actuator in the module is paired to a valve and dedicated channel of a communication IC. A common pneumatic supply line provides fluid power to every module simultaneously, whereas a common electrical bus similarly provides electrical power. (**C**) Control commands are assembled into data packets by a main controller and relayed by the IC through each module connected in series. Each module has three independent channels (X, Y, and Z) that can be addressed to control up to three embedded valves in open loop.

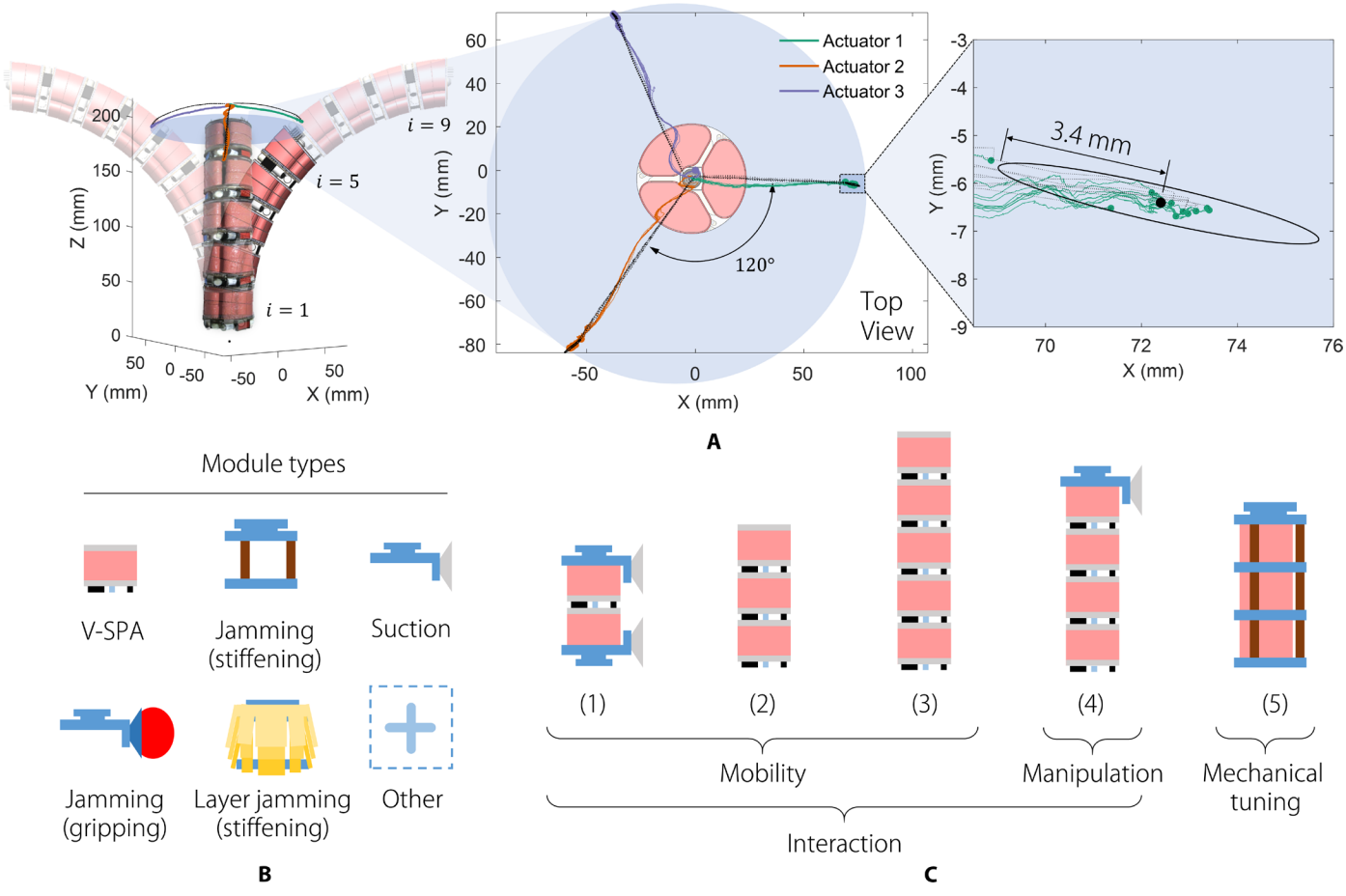

Fig. 4. Versatility of vacuum-powered soft hyper-redundant robot. The workspace and repeatability of the five-module soft hyper-redundant robot is depicted in (**A**) along with a depiction of the maximum reach for up to nine modules. To measure the range of motion along three primary directions determined by the actuators in each module, three markers were placed on the top of the distal module, and a centroid was calculated to track the center of the module as the robot end point. A top view of the distal module centroid 3D trajectory is shown through a 10-cycle repeatability test. A variety of module types shown in (**B**) can be readily integrated with the hyper-redundant robot. The configurations in (**C**) combining various modules are all validated experimentally in subsequent sections.

in part to variable actuator functionality in response to load, this can also be a factor of the robot design, which included a passive DoF at the lower foot needed for climbing and an offset of the payload mass resulting in a moment that pulled the robot away from the wall and reduced step size.

Interaction task: Multimodal locomotion

Alternate modes of locomotion were also found to be possible using the modular vacuum-driven soft continuum robot system suitable for potential use in diverse and variable environments. Up to five V-SPA Modules were assembled in series and programmed to achieve two distinct gaits following strategies investigated previously for continuum style snake robots (*45*–*47*): a wave gait and a rolling gait. The first of these is shown with a sequence of video frames in Fig. 5B depicting the progression of the forward wave gait over a flat, level surface with a measured average speed of 5 mm/s (0.05 BL/s). As a secondary but inherited feature of the modular robot structure, the reconfigurability and robustness of the continuum robot are also exhibited in Fig. 5C, where locomotion is preserved [and even improved in terms of average speed, measuring 11 mm/s (0.08 BL/s)] after two modules were removed from the robot, without requiring any changes to the gait controller. The increase in speed results only from an inherent change in vacuum supply air flow, which is restricted more for every module attached. Better designs could compensate for this by providing a central supply line with larger diameter.

Lateral motion was also accomplished using a rolling gait, expanding the utility of the mobile robot to suit different locomotion objectives. This gait, shown in Fig. 5D, is capable of much higher locomotion speeds (an average speed of 60 mm/s or 1.33 BL/s) than the wave gait of any robot length; however, this is possible only at the cost of a larger operational workspace (wider body span relative to the direction of travel). In practice, the multimodal functionality of this type of robot may be exploited to achieve fast motion over generally wide, open terrain using the rolling gait, whereas slower, cautious navigation through narrow passages, gaps, or obstructions could be approached using the wave gait, which operates within a more slender body width. A demonstration of the continuum robot gaits described can be found in movie S6.

Mechanical tuning: Jamming-based stiffening

Although our initial workspace testing indicated that the compliance of the arm does not significantly affect repeatability, manipulation testing of the soft arm, as well as experience from literature (*48*), reveals that the controllability of such a soft structure to precise locations

remains a challenge. This was apparent from qualitative observations of object manipulation/relocation tasks, where the object mass in addition to the inertia of the arm itself led to oscillatory behavior. Although closing the active control loop to better maintain positioning and path following is likely needed for the best results, these tasks would benefit from other methods of "passive control," including the ability to tune mechanical system parameters of soft robotic devices themselves. In particular, this motivated the design and integration of a peripheral variable stiffness module to provide the ability to change the overall rigidity or passivity of the soft arm.

Distributed across the length of the continuum robot arm, this module is composed of multiple stiffening pillars in parallel with each actuator module and uses jamming of enclosed granular media (ground coffee) driven by actively controlled vacuum to vary the stiffness of the overall structure. Figure 6 shows the resulting stiffness characteristics of the soft continuum robot fitted with the stiffening module when force is applied through a high-strength nylon thread (fishing line) at the distal module perpendicular to the axis of the vertically mounted robot. Jamming pillars were spaced in three columns around each V-SPA Module and powered together with 88.5% vacuum when activated. The tested directions are grouped as either a pull in the direction of a jamming column, toward the vertex of the triangle formed from a top view of the three columns, or toward an edge, between two jamming columns. Five cycles were performed in each direction, with the result for each condition provided as an average of these trials. The measurements indicate an increase of stiffness in every direction when jamming is enabled, with the greatest increase always in the direction of a vertex, and hence the most direct compression of a single jamming column, with increases of 38.8, 48.5, and 31.7% when vacuum is applied versus when it is not. In the direction of an edge, the stiffness was only moderately increased from their activation, by 15.1, 31.5, and 17.3% for the three edge direction loading conditions. A diagram of the test setup is shown in fig. S2, along with a depiction of the fabrication process used to produce the granular jamming units.

The jamming modules in this demonstration are coupled and joined to the same controlled vacuum input but could equally be included as part of more advanced actuator modules with internally integrated, independently controlled jamming pillars for more selective mechanical tuning capability of a soft structure. In addition, only granular jamming was explored for this investigation of mechanical tuning, but stiffening with vacuum can also be achieved using flexible sheet materials sandwiched between air-sealed plastic film to achieve similar or possibly improved results (*30*, *49*).

DISCUSSION

The actuators presented here and the combined example applications illustrate the versatility of vacuum-based SPAs constructed from simple materials and methods. The fabrication procedure for V-SPAs reduces the time, tools, and cost required for creating actuators for soft robots by using only 2D manufacturing methods and eliminating conventional molds, which allows rapid, batch production from minimal effort in comparison with other SPA types. Although conventional molding techniques inherently produce more uniform actuator structure and reduced variability between different actuators, the accuracy and repeatability of individual V-SPAs are not significantly affected as shown here, despite the variable wall thickness produced from manual application of silicone rubber layers. This improvement in actuator fabrication serves to decrease the design and development cycle time, leaving more room for focus on the system-level development of complete and useful soft robots. Toward the same goal, the use of vacuum as a primary pneumatic supply source to power V-SPAs enables more efficient integration of other vacuum-based mechanisms in a single soft robotic system, allowing for more complex and diverse soft robot capability. This potential was effectively demonstrated through the use of modular units, which allow many vacuum-driven mechanisms, as well as many redundant actuators, to be seamlessly combined and tested in different soft robot configurations. Furthermore, unlike most other SPAs (*6*–*16*), using a single source of pneumatic power significantly reduces the overhead cost of redundant subsystem infrastructure needed in comparison with the alternative case, where components—such as regulators, distribution manifolds, and central supply lines—cannot be shared. This simplification saves weight and design effort.

V-SPAs likewise support the implementation of systems with many active DoFs, through the use of lightweight foam material as a central component,

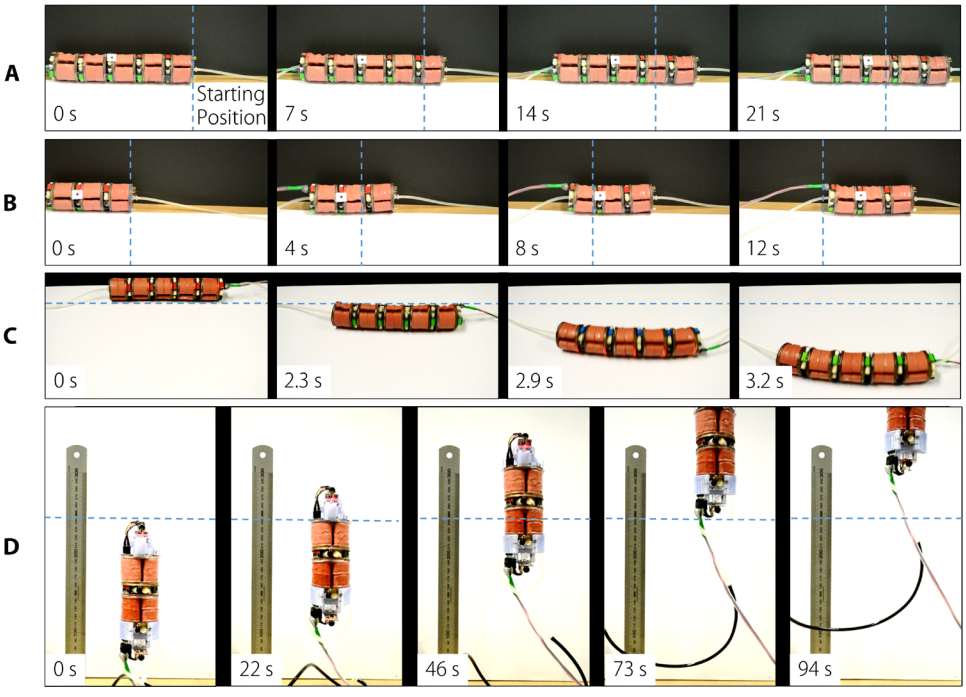

Fig. 5. Diverse locomotion modes of modular continuum robot. A series of frames captured from video is shown for each of the four different gait modes: wave gait with five V-SPA Modules (**A**), wave gait with three V-SPA Modules (**B**), rolling gait (**C**), and vertical climbing with suction cup modules (**D**).

helping to significantly reduce the weight cost of additional actuation. In combination with plug-and-play architecture, this enables systems such as those demonstrated here with up to 15 actuators or with fewer DoFs and available payload capacity to support future integration of onboard batteries and power generation. Both of these aspects represent current goals and challenges of research in the soft robotics field toward real-world application of the newly forming technologies coming from within it.

Although the advantages of foam V-SPAs are promising for the development of a new type of complex soft robots, they are not without certain fundamental and practical limits. The capacity of vacuum to produce useful contractile work in an actuator is limited by the pressure of its external environment. For nominal use at standard atmospheric pressure, this serves as an absolute limitation; however, in more creative applications such as use in alternative environments (underwater or exoplanetary), this "limit" can be treated as a parameter to be considered in design. In any case, for a given setting, this coupling to the environment imposes a boundary on the performance of the actuators and hence the system as a whole. Beyond this inherent physical limit, the specific design implementation of V-SPAs in soft robotic systems can also be seen as a limitation, because the actuators do not provide a consistent mechanical constraint alone to direct their motion unless used carefully. Although the 2D manufacturing method used here can be adapted to allow for more complex shapes conducive to directed buckling (bellows-like shapes) and actuation, the most effective method for this is through the support of external constraints, such as reliance on the stiffness of an attached surface to restrict the buckling of the actuator along that interface, allowing it to occur only between two moving bodies as desired. In addition, external structures can help impose constraints and define actuator motion, such as the stiffness of other coupled actuators or as a well-defined joint axis of rotation (see movie S1). The rigid upper and lower plates, as well as the flexible but nonstretchable central conduit of the V-SPA Modules produced here, serve these purposes in part, ensuring that the contraction of the actuators results primarily in rotational motion.

The simplicity of this V-SPA concept encourages the development of even more creative techniques and applications for soft actuation. Other methods of elastic foam production could be used in the future to create complex 3D structures, possibly deviating from the strict use of off-the-shelf materials. Variable stiffness skin components of either different thicknesses or material could be used to generate more complex actuation patterns for increasingly advanced V-SPA designs using multimaterial 3D printers or other standard soft robot fabrication tools. Regardless of the implementation method or application, future soft robots will benefit from exploring and exploiting the benefits of both foam-based materials

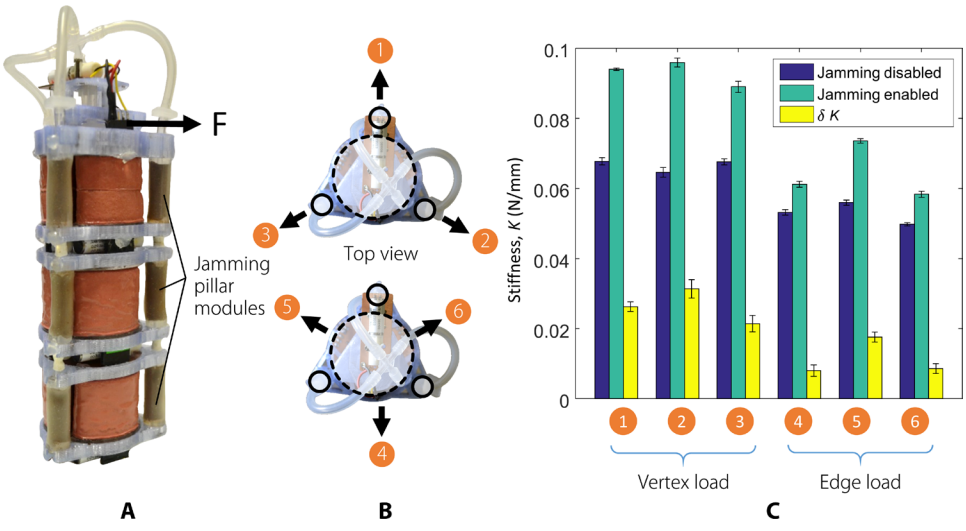

Fig. 6. Granular cellular matrix jamming enables active stiffness tuning of vacuum-driven soft structures. (**A**) The addition of a jamming module enables stiffening of a continuum robot composed of three V-SPA Modules. The stiffness was measured using a vertical material testing machine, configured with a grounded pulley to redirect vertical motion of a cable to the horizontal direction. Tensile force and displacement measured in the vertical direction were thereby mapped to the direction perpendicular to the initially vertical axis of the actuator structure. (**B**) The cable was attached at the top of the distal module, and the assembly was rotated in increments of 60° to six total positions for measurements in multiple radial directions, with five loading cycles performed in each position. The measured stiffness shown in (**C**) increased in every direction when the jamming module was activated, in comparison with its inactive state. Error bars represent 1 SD.

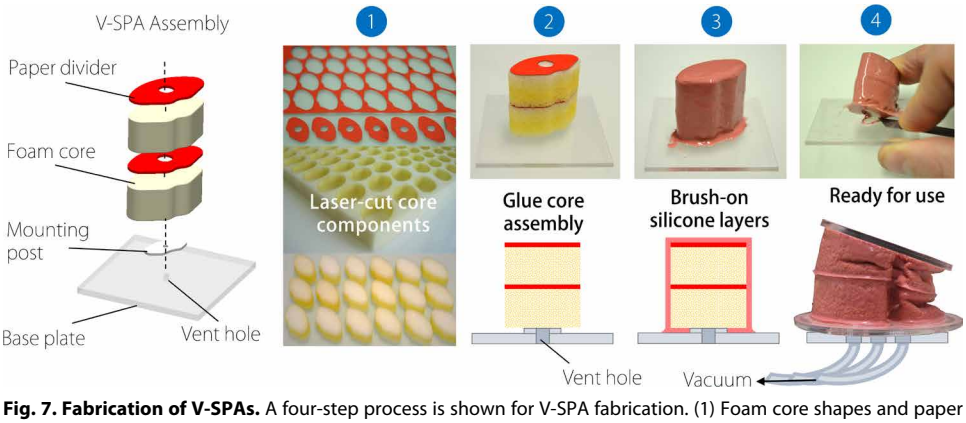

Fig. 7. Fabrication of V-SPAs. A four-step process is shown for V-SPA fabrication. (1) Foam core shapes and paper divider plates were cut using a computer numerical control (CNC) CO_2 laser. (2) Actuator cores and dividers were assembled on a mounting post of a preform structure using cyanoacrylate gel. (3) Two coats of silicone rubber were applied to the outer surface of the foam core assembly, including the space between the bottom foam and base plate. A vent hole is included through the mounting post and base plate to reduce the formation of bubbles caused by expanding internal air in the foam core when a heating oven is used to speed curing. Layer cure was allowed between coats. (4) The actuator was removed from the preform using a razor to separate the attached foam and finally glued to a vacuum distribution manifold.

and vacuum power as new viable means to achieving versatile capabilities for environmental interaction and controlled modulation of mechanical system performance.

MATERIALS AND METHODS

Objectives

The objective of this study was to characterize and validate the performance and integration of V-SPAs in multifunctional vacuum-based soft robots. We explain the design procedure and fabrication techniques for the actuators and multi-DoF actuator modules, and describe test methods for obtaining performance metrics for each.

Actuator design and fabrication

The fabrication process of a V-SPA shown in Fig. 7 begins with a basic preform structure, to act as a mount during application of the outer rubber layer and as a mask over the foam where connection of a vacuum supply to the internal actuator cavity is eventually made. For the actuators produced here, the preform also served to create a smooth flat surface on the same side as the supply access mask when peeled off, so the actuator will form a good seal when glued to an equally smooth flat supply distribution plate.

The actuator itself is composed of 2D foam core shapes manufactured from a sheet of open-celled polyurethane foam (12.7-mm-thick polyurethane foam, McMaster-Carr, 8643K511) and rigid paper dividers. The porous foam cores serve as the main actuator body, whereas the paper dividers help reduce the buckling on the upper surface of the actuator and, at intervals along the height, enforce deformation primarily in the vertical direction. A CO_2 laser was used to cut many foam core and paper divider components from a single sheet at once, allowing batch production of the actuators. The foam cores and paper dividers are assembled in a stack with cyanoacrylate gel glue and then glued to the preform. After preparation by mixing and degassing, two coats of ELASTOSIL M 4601 silicone rubber (Wacker Chemie AG) are spread with brush-like strokes onto all exposed surfaces of the foam core using a flexible spreader (thin cardboard) while being cured at 50°C between coats. Once cured, the actuators can be removed from the preform and attached to a vacuum supply or used directly on the preform by applying vacuum to the vent hole through the base.

Although the basic construction of V-SPAs is described above, many variable parameters affect actuator performance. One of the leading design variables is geometry, because it pertains to dimensions that are easy to change, like actuator shape, and to others that are more difficult to manipulate, like the porosity of the foam used. As a starting point, we investigated only minor changes in actuator morphology toward a very specific goal—to create a circular module with three actuators and room at the center to pass wiring and a central pneumatic supply. This bounded the overall shape of the actuator to be used, but small improvements were added in an effort to achieve specific behaviors and subjectively improved performance criteria, in this case maximal linear deflection. To increase the directionality of the actuators, we selected a particular geometry for the foam core that would allow inward compression and buckling of sidewalls without interference limiting the downward actuator stroke. This helped to direct actuator contraction to the axial direction, perpendicular to the top plane of the original foam sheet. Then, multiple foam chambers were created by stacking individual foam cores to increase the actuator range of motion. To create independent porous volumes within a single actuator, we assembled thin 0.2-mm heavy-gauge paper dividers between two foam cores glued together in a stack to form an internal membrane. The dividers contain a 6-mm hole at the center to allow air flow between chambers while still enforcing separation. Without this membrane, the overall structure of the two-core actuators would yield an effectively taller actuator, which, for the same given cross-sectional area, would yield a more horizontal than vertical mode of collapse upon vacuum activation. Although a parametric study was not conducted to properly determine an ideal V-SPA compression ratio, it is plausible that an optimal relationship exists to best select actuator height based on cross-sectional geometry (aspect ratio) for linear actuation. For planar fabrication methods, this ratio is the most accessible parameter to optimize; however, an ideal actuator shape would incorporate geometric contours along the "walls" of the foam core to increase stress concentrations for uniform buckling, much in the same way a corrugated bellows collapses. This is partly achieved by creating multichamber actuators, whose stiff dividers act similarly to limit the stress along designated rings around the actuator perimeter. A separate study could investigate the optimal size and number of separate foam core chambers needed to maximize deflection or force using this design method.

Other factors—including foam type and composition, porosity, and elastomer coating material—are expected to greatly affect the performance of V-SPAs, but the methods for testing these variations involve greater effort. To begin, different foam materials and elastomers behave differently, and not all combinations allow for full curing of multi-part elastomers that chemically interact. Open-cell foam materials of different composition and porosity are also limited as off-the-shelf components but can be produced from scratch for testing if desired. These factors limit the possibility for ready empirical parameterization testing. Perhaps a more controlled and available approach would be to simulate the effect and performance of actuator deformation using finite element modeling techniques, but this proves to be difficult and holds no greater advantage: Accurate models of this type still require empirical testing to determine material property values. Nevertheless, as data and models improve over time, this technique will prove to be invaluable as actuators, such as the V-SPA, are adopted for further use.

The use of primarily off-the-shelf materials allows this new type of actuator to be easily produced with low resources, partly to extend the accessibility and scope of soft robot construction and research, especially toward the realm of lower education STEM (science, technology, engineering, and mathematics) outreach programs. However, the concept of foam vacuum actuation is not exclusively tied to these materials and methods of manufacture. We capitalized greatly from laser-cutting machines for fabricating 2D foam core shapes, but this tool is not required and virtually any method for cutting foam sheets will suffice. Early prototypes of V-SPAs were built from scissor-cut foam cores attached to the end of wooden dowels (to serve as a mount and mask) and could be directly super-glued to a supply tube with the outer rubber skin used to seal the foam and fix the tube to the actuator in a single step. As an alternative to brushing on the outer rubber layer, dipping might also be used to coat an entire foam core for even faster manufacture time.

V-SPA Module control and characterization

Control of each V-SPA Module connected in series is achieved over a single-wire interface, enabled by a low-cost and readily available integrated circuit (IC) originally designed for controlling individual

LED pixels in networked displays (Worldsemi, WS2811). The IC is repurposed to supply an activation signal to onboard amplifiers for direct control over three embedded solenoid valves (Lee, LHDA0531115H) shadowing the operation of each color channel of an RGB LED. A significant benefit of this IC is that it tolerates real-time reconfiguration of hardware, enabling plug-and-play functionality of the V-SPA Modules. Robots can therefore be reduced or extended fundamentally to any number of modules on a single bus over relatively large spans, with only practical limitations imposed by random-access memory (RAM) and electrical power required. With standard microcontrollers, such as Arduino, hundreds of IC-enabled modular units can be controlled in a serial network through a single wire with little additional local electronics hardware, compared with alternative networking schemes (I2C, CAN, and direct serial), which require more local computational power. Figure 4B depicts the topology of this network architecture, whereas a schematic of the internal electronic connections to the LED driver IC can be seen in fig. S3.

To determine the performance characteristics of a V-SPA Module, we empirically measured a step response for multiple values across different conditions. Each response was averaged from three different actuators, cycled 10 times each. This process was repeated for 10 conditions of varying load and 10 conditions of varying input vacuum. Load was applied by calibrated weights through a cable hung over a pulley and attached to a short lever arm fixed to the module. Vacuum pressure was varied by changing the positive supply pressure to a vacuum ejector module (SMC ZH05B). The cycles for all three actuators in each condition were averaged to obtain a single representative step response curve from which performance metrics were extracted. The maximum angular motion is directly measured, whereas the rise time is found from the time between response crossings at 10 and 90% of the maximum angular deflection. The initial angular velocity is also found in this region, from a linear fit to the first half of the actuator motion (up to 50%), where the response curve is dominantly linear.

Blocked moment measurements of the V-SPA Module were obtained using a six-axis force and torque sensor (Nano17 SI-25-0.25, ATI Industrial Automation) mounted to the upper plate of the module constrained at the base in a rigid test fixture. The reported value was averaged from individual activation of three different actuators, cycled 10 times each. With an alternate setup, the average mechanical power output of a V-SPA Module was also estimated through measurements of displacement, Δh, and time, Δt, for a known mass, m, fixed to a cable hung over a pulley (assumed to be a constant force, $F = mg$), and driven by a short arm attached to the module, following $P = F \cdot \Delta h/\Delta t$. The metrics of torque and power were normalized by the mass of the module and the actuator alone to compute specific torque (τ_s), specific power (P_s), and specific energy (E_s). Although the latter of these is relatively low compared with other vacuum-powered actuators (*20*), with $P_s = 5$ W kg^{-1} and $E_s = 1.2$ J kg^{-1}, the value of specific torque is found to be relatively high, with $\tau_s = 45.3$ N·m kg^{-1} (45.3 N·mm g^{-1}), more than five times that of the modular dc motor–powered actuators designed for a conventional rigid continuum robot, the Unified Snake (*50*).

SUPPLEMENTARY MATERIALS

robotics.sciencemag.org/cgi/content/full/2/9/eaan6357/DC1
Fig. S1. Anatomy of a V-SPA.
Fig. S2. Fabrication and testing of jamming module.
Fig. S3. Single wire module networking with serial LED driver IC.
Movie S1. Binary control of 3-DoF V-SPA array without modular interface.
Movie S2. Binary workspace of V-SPA Module.
Movie S3. Continuum robot repeatability test.
Movie S4. Vacuum suction manipulation with continuum robot.
Movie S5. Vacuum suction climbing with payload.
Movie S6. Vacuum robot locomotion.
Reference (*51*)

REFERENCES AND NOTES

1. R. Ikeura, H. Inooka, Variable impedance control of a robot for cooperation with a human, in *Proceedings of the 1995 IEEE International Conference on Robotics and Automation* (IEEE, 1995), pp. 3097–3102.
2. A. Calanca, R. Muradore, P. Fiorini, Impedance control of series elastic actuators using acceleration feedback, in *Wearable Robotics: Challenges and Trends* (Springer, 2017), pp. 33–37.
3. R. Pfeifer, M. Lungarella, F. Iida, Self-organization, embodiment, and biologically inspired robotics. *Science* **318**, 1088–1093 (2007).
4. R. Pfeifer, M. Lungarella, F. Iida, The challenges ahead for bio-inspired 'soft' robotics. *Commun. ACM* **55**, 76–87 (2012).
5. C. Laschi, B. Mazzolai, M. Cianchetti, Soft robotics: Technologies and systems pushing the boundaries of robot abilities. *Sci. Robot.* **1**, eaah3690 (2016).
6. K. C. Galloway, P. Polygerinos, C. J. Walsh, R. J. Wood, Mechanically programmable bend radius for fiber-reinforced soft actuators, in *Proceeding of the 2013 16th International Conference on Advanced Robotics (ICAR)* (ICAR, 2013), pp. 1–6.
7. M. A. Robertson, H. Sadeghi, J. M. Florez, J. Paik, Soft pneumatic actuator fascicles for high force and reliability. *Soft Robot.* **4**, 23–32 (2016).
8. P. Moseley, J. M. Florez, H. A. Sonar, G. Agarwal, W. Curtin, J. Paik, Modeling, design, and development of soft pneumatic actuators with finite element method. *Adv. Eng. Mater.* **18**, 978–988 (2016).
9. G. Agarwal, N. Besuchet, B. Audergon, J. Paik, Stretchable materials for robust soft actuators towards assistive wearable devices. *Sci. Rep.* **6**, 34224 (2016).
10. D. Rus, M. T. Tolley, Design, fabrication and control of soft robots. *Nature* **521**, 467–475 (2015).
11. A. D. Marchese, R. K. Katzschmann, D. Rus, A recipe for soft fluidic elastomer robots. *Soft Robot.* **2**, 7–25 (2015).
12. G. Krishnan, J. Bishop-Moser, C. Kim, S. Kota, Kinematics of a generalized class of pneumatic artificial muscles. *J. Mech. Robot.* **7**, 041014 (2015).
13. B. Tondu, Modelling of the McKibben artificial muscle: A review. *J. Intell. Mater. Syst. Struct.* **23**, 225–253 (2012).
14. B. Mosadegh, P. Polygerinos, C. Keplinger, S. Wennstedt, R. F. Shepherd, U. Gupta, J. Shim, K. Bertoldi, C. J. Walsh, G. M. Whitesides, Pneumatic networks for soft robotics that actuate rapidly. *Adv. Funct. Mater.* **24**, 2163–2170 (2014).
15. H. A. Sonar, J. Paik, Soft pneumatic actuator skin with piezoelectric sensors for vibrotactile feedback. *Front. Robot. AI* **2**, 38 (2016).
16. A. Firouzeh, M. Salerno, J. Paik, Soft pneumatic actuator with adjustable stiffness layers for multi-DoF actuation, in *Proceedings of the 2015 IEEE/RSJ International Conference on Intelligent Robots and Systems (IROS)* (IEEE, 2015), pp. 1117–1124.
17. C. Eppner, R. Deimel, J. Álvarez-Ruiz, M. Maertens, O. Brock, Exploitation of environmental constraints in human and robotic grasping. *Int. J. Robot. Res.* **34**, 1021–1038 (2015).
18. M. T. Tolley, R. F. Shepherd, B. Mosadegh, K. C. Galloway, M. Wehner, M. Karpelson, R. J. Wood, G. M. Whitesides, A resilient, untethered soft robot. *Soft Robot.* **1**, 213–223 (2014).
19. F. Ilievski, A. D. Mazzeo, R. F. Shepherd, X. Chen, G. M. Whitesides, Soft robotics for chemists. *Angew. Chem. Int. Ed.* **50**, 1890–1895 (2011).
20. D. Yang, S. M. Verma, J.-H. So, B. Mosadegh, C. Keplinger, B. Lee, F. Khashai, E. Lossner, Z. Suo, G. M. Whitesides, Buckling pneumatic linear actuators inspired by muscle. *Adv. Mater. Technol.* **1**, 1600055 (2016).
21. D. Yang, M. S. Verma, E. Lossner, D. Stothers, G. M. Whitesides, Negative-pressure soft linear actuator with a mechanical advantage. *Adv. Mater. Technol.* **2**, 1600164 (2017).
22. B. C. Mac Murray, X. An, S. S. Robinson, I. M. van Meerbeek, K. W. O'Brian, H. Zhao, R. F. Shepherd, Poroelastic foams for simple fabrication of complex soft robots. *Adv. Mater.* **27**, 6334–6340 (2015).
23. A. Argiolas, B. C. Mac Murray, I. Van Meerbeek, J. Whitehead, E. Sinibaldi, B. Mazzolai, R. F. Shepherd, Sculpting soft machines. *Soft Robot.* **3**, 101–108 (2016).
24. I. M. Van Meerbeek, B. C. Mac Murray, J. W. Kim, S. S. Robinson, P. X. Zou, M. N. Silberstein, R. F. Shepherd, Morphing metal and elastomer bicontinuous foams for reversible stiffness, shape memory, and self-healing soft machines. *Adv. Mater.* **28**, 2801–2806 (2016).
25. B. Trimmer, Soft robots and size. *Soft Robot.* **2**, 49–50 (2015).
26. E. Brown, N. Rodenberg, J. Amend, A. Mozeika, E. Steltz, M. R. Zakin, H. Lipson, H. M. Jaeger, Universal robotic gripper based on the jamming of granular material. *Proc. Natl. Acad. Sci. U.S.A.* **107**, 18809–18814 (2010).

27. F. Tramacere, M. Follador, N. M. Pugno, B. Mazzolai, Octopus-like suction cups: From natural to artificial solutions. *Bioinspir. Biomim.* **10**, 035004 (2015).
28. Y.-J. Kim, S. Cheng, S. Kim, K. Iagnemma, A novel layer jamming mechanism with tunable stiffness capability for minimally invasive surgery. *IEEE Trans. Robot.* **29**, 1031–1042 (2013).
29. N. G. Cheng, M. B. Lobovsky, S. J. Keating, A. M. Setapen, K. I. Gero, A. E. Hosoi, K. D. Iagnemma, Design and analysis of a robust, low-cost, highly articulated manipulator enabled by jamming of granular media, in *Proceedings of the 2012 IEEE International Conference on Robotics and Automation (ICRA)* (IEEE, 2012), pp. 4328–4333.
30. J. L. C. Santiago, I. D. Walker, I. S. Godage, Continuum robots for space applications based on layer-jamming scales with stiffening capability, in *Proceedings of the 2015 IEEE Aerospace Conference* (IEEE, 2015), pp. 1–13.
31. M. Cianchetti, R. Tommaso, G. Giada, N. Thrishantha, A. Kaspar, D. Prokar, M. Arianna, Soft robotics technologies to address shortcomings in today's minimally invasive surgery: The STIFF-FLOP approach. *Soft Robot.* **1**, 122–131 (2014).
32. W. McMahan, V. Chitrakaran, M. Csencsits, D. Dawson, I. D. Walker, B. A. Jones, M. Pritts, D. Dienno, M. Grissom, C. D. Rahn, Field trials and testing of the OctArm continuum manipulator, in *Proceedings of the 2006 IEEE International Conference on Robotics and Automation* (ICRA, 2006), pp. 2336–2341.
33. P. Qi, C. Qiu, H. Liu, L. D. Seneviratne, K. Althoefer, A novel continuum manipulator design using serially connected double-layer planar springs. *IEEE/ASME Trans. Mechatronics* **21**, 1281–1292 (2016).
34. M. W. Hannan, I. D. Walker, The 'elephant trunk' manipulator, design and implementation, in *Proceedings of the 2001 IEEE/ASME International Conference on Advanced Intelligent Mechatronics* (IEEE, 2001), pp. 14–19.
35. K. Suzumori, S. Iikura, H. Tanaka, Development of flexible microactuator and its applications to robotic mechanisms, in *Proceedings of the 1991 IEEE International Conference on Robotics and Automation* (IEEE, 1991), pp. 1622–1627.
36. G. S. Chirikjian, thesis, California Institute of Technology, Pasadena, CA (1992).
37. J. Burgner-Kahrs, D. C. Rucker, H. Choset, Continuum robots for medical applications: A survey. *IEEE Trans. Robot.* **31**, 1261–1280 (2015).
38. H. Marvi, C. Gong, N. Gravish, H. Astley, M. Travers, R. L. Hatton, J. R. Mendelson III, H. Choset, D. L. Hu, D. I. Goldman, Sidewinding with minimal slip: Snake and robot ascent of sandy slopes. *Science* **346**, 224–229 (2014).
39. B. Bayat, A. Crespi, A. Ijspeert, Envirobot: A bio-inspired environmental monitoring platform, in *Proceedings of the IEEE/OES Conference on Autonomous Underwater Vehicles (AUV)* (IEEE, 2016), pp. 381–386.
40. S. Hirose, *Biologically Inspired Robots: Serpentile Locomotors and Manipulators* (Oxford Univ. Press, 1993).
41. A. A. Stokes, R. F. Shepherd, S. A. Morin, F. Ilievski, G. M. Whitesides, A hybrid combining hard and soft robots. *Soft Robot.* **1**, 70–74 (2013).
42. P. Liljebäck, Ø. Stavdahl, K. Y. Pettersen, Modular pneumatic snake robot: 3D modelling, implementation and control. *Model. Identif. Control Nor. Res. Bull.* **29**, 21–28 (2008).
43. C. D. Onal, D. Rus, Autonomous undulatory serpentine locomotion utilizing body dynamics of a fluidic soft robot. *Bioinspir. Biomim.* **8**, 026003 (2013).
44. G. Gerboni, T. Ranzani, A. Diodato, G. Ciuti, M. Cianchetti, A. Menciassi, Modular soft mechatronic manipulator for minimally invasive surgery (MIS): Overall architecture and development of a fully integrated soft module. *Meccanica* **50**, 2865–2878 (2015).
45. J. Dai, M. Travers, T. Dear, C. Gong, H. C. Astley, D. I. Goldman, H. Choset, Robot-inspired biology: The compound-wave control template, in *Proceedings of the 2015 IEEE International Conference on Robotics and Automation (ICRA)* (IEEE, 2015), pp. 5879–5884.
46. K. Melo, L. Paez, Experimental determination of control parameter intervals for repeatable gaits in modular snake robots, in *Proceedings of the 2014 IEEE International Symposium on Safety, Security, and Rescue Robotics (SSRR)* (IEEE, 2014), pp. 1–7.
47. M. Mori, S. Hirose, Three-dimensional serpentine motion and lateral rolling by active cord mechanism ACM-R3, in *Proceedings of the IEEE/RSJ International Conference on Intelligent Robots and Systems* (IEEE, 2002), pp. 829–834.
48. M. Manti, V. Cacucciolo, M. Cianchetti, Stiffening in soft robotics: A review of the state of the art. *IEEE Robot. Autom. Mag.* **23**, 93–106 (2016).
49. J. Ou, L. Yao, D. Tauber, J. Steimle, R. Niiyama, H. Ishii, jamSheets: Thin interfaces with tunable stiffness enabled by layer jamming, in *Proceedings of the 8th International Conference on Tangible, Embedded and Embodied Interaction TEI '14* (ACM, 2014), pp. 65–72.
50. C. Wright, A. Buchan, B. Brown, J. Geist, M. Schwerin, D. Rollinson, M. Tesch, H. Choset, Design and architecture of the unified modular snake robot, in *Proceedings of the 2012 IEEE International Conference on Robotics and Automation* (IEEE, 2012), pp. 4347–4354.
51. adafruit/Adafruit_NeoPixel, https://github.com/adafruit/Adafruit_NeoPixel.

Acknowledgments: We thank A. Wu (École Polytechnique Fédérale de Lausanne) for assistance with motion capture and data processing and K. Melo (KM-RoBoTa) for counsel on the subject of snake robotics, which greatly improved this manuscript. **Funding:** This work was supported by the Swiss National Science Foundation Fund for RoBuSt project (513836) and the Swiss National Centre of Competence in Research Robotics. **Author contributions:** M.A.R. conceived the concepts, designed and built the hardware, designed and conducted experiments, analyzed data, and wrote the manuscript. J.P. developed the concepts, directed the research, designed the experiments, and edited the manuscript. **Competing interests:** The author declare that they have no competing interests. **Data and materials availability:** Contact J.P. for any questions regarding EAGLE CAD files, schematics, and parts list for electrical components; Solidworks CAD models for a single V-SPA Module assembly with dimensions as fabricated here; and for experimental raw data and processing scripts.

Submitted 11 May 2017
Accepted 8 August 2017
Published 30 August 2017
10.1126/scirobotics.aan6357

Citation: M. A. Robertson, J. Paik, New soft robots really suck: Vacuum-powered systems empower diverse capabilities. *Sci. Robot.* **2**, eaan6357 (2017).

Science Robotics

New soft robots really suck: Vacuum-powered systems empower diverse capabilities

Matthew A. Robertson and Jamie Paik

Sci. Robot. **2** (9), eaan6357. DOI: 10.1126/scirobotics.aan6357

Science Robotics (ISSN 2470-9476) is published by the American Association for the Advancement of Science. 1200 New York Avenue NW, Washington, DC 20005. The title *Science Robotics* is a registered trademark of AAAS.